

## A FINITE ELEMENT METHOD FOR THE EDDY CURRENTS PROBLEM IN AN ELECTRODE WITH INPUT INTENSITIES AS BOUNDARY DATA

Alfredo Bermúdez\*, Rodolfo Rodríguez†, and Pilar Salgado\*

\*Departamento de Matemática Aplicada  
Universidade de Santiago de Compostela  
15706, Santiago de Compostela, Spain  
e-mail: mabermud@usc.es, mpilar@usc.es

†GI<sup>2</sup>MA  
Departamento de Ingeniería Matemática  
Universidad de Concepción  
Casilla 160-C, Concepción, Chile  
e-mail: rodolfo@ing-mat.udec.cl  
web page: <http://lanin.ing-mat.udec.cl/~rodolfo/>

**Key Words:** Eddy currents, non-standard boundary data, Lagrange multipliers.

**Abstract.** *The aim of this paper is to introduce a finite element method to solve the eddy currents model in a bounded conductor domain. In particular we study a weak formulation in terms of the magnetic field. In order to impose suitable boundary conditions from a physical point of view, we introduce a Lagrange multiplier defined on the boundary and study the resulting mixed formulation by using classical techniques.*

## 1 INTRODUCTION

Numerical solution of the eddy currents model became an important research area in recent years because of many applications in electrical engineering (see for instance [1] and references therein). In particular, the present work is motivated by the need of a three-dimensional numerical simulation of metallurgical electrodes in an electric arc furnace (see for instance [2, 3] for related works concerning axisymmetric models).

Electrodes are among the main components of reduction furnaces for ferro-alloys, calcium carbide, iron and some others. Their purpose is to generate high temperatures which are needed for the reduction chemical reactions to take place. For this, a great amount of energy is generated in an electric arc which arises on the tip of each electrode at the furnace center (Si, FeSi processes), or in a resistive layer (slag processes).

Typical diameter of electrodes is 1-2 m while their length is of the order of 10 m. High intensity alternating electric current up to 150 kA is used. Classical electrodes extensively used in industry include pure graphite, prebaked and Soderberg electrodes. The latter are built of paste consisting of a carbon aggregate and a tar binding which are fed into a steel casing. A number of steel fins are attached to the inside of the casing. The great amount of heat generated by Joule effect is partially employed for baking the paste. This is a crucial process during which the initially soft/liquid non-conductive paste at the top of the electrode becomes a solid carbon conductor. Accordingly, its electrical conductivity undergoes important changes along the electrode. In fact, it depends on temperature because the latter determines the baking process. As a consequence it is of great importance to get a correct temperature distribution. In particular the position of the baking zone strongly influences the electrode operation.

The advantages of Soderberg electrodes with respect to pure graphite or prebaked electrodes are that they are built in larger sizes and cost less. However, as the electrode is consumed, it has to be slipped typically 0.5 m per day. Then the casing melts and pollutes the final product and this is why they cannot be used for silicon metal. In fact, for silicon furnaces prebaked electrodes were the only alternative used until this decade.

Recently (see [4]) a new compound electrode for the production of silicon has been developed by Ferroatlántica Company in Spain. It consists of a central column of baked carbonaceous material, graphite or similar, which acts as a central mechanical support and an outside steel casing with the same diameter as the prebaked electrodes currently in use. A special Soderberg paste is introduced between the central column and the casing which flows down the column until it finishes baking in the area of the contact clamps through which the electric current is introduced.

Two different slipping systems exist, one for the casing and another one for the central column; the combination of both systems is necessary so as to slip the casing as little as possible and also to carry out the correct extrusion of the carbon electrode with the central column slipping rings.

The result is that the furnace works in a completely similar way to those including

prebaked electrodes and there is no appreciable pollution in the silicon due to the casing. Unlike standard Soderberg electrodes, the casing does not have fins which are needed to bake the paste more easily. Actually the inside of the casing is absolutely smooth so as to allow the slippage of the electrode throughout the casing. The casing is really an extrusion sleeve.

However, its overall thermo-electrical behavior changes with respect to pure Soderberg or prebaked electrodes. The reason is that graphite is a better conductor than Soderberg paste so, in particular, the skin effect is less important than in pure graphite, prebaked or classical Soderberg electrodes.

The main advantage of these compound electrodes is decreasing cost. In silicon metal production saving is around 12-16%. One inconvenience is that the slipping velocity is not free as it is for prebaked electrodes because paste has to be baked and this need a minimum period of time between slipping. In fact the baking of paste is a crucial point in the working of this type of electrode and mathematical models can help us to know the position of the baked/non-baked interphase.

In general, whatever the type of electrodes we consider, the great complexity in designing and operating them makes it very convenient to use numerical simulation to predict their behavior. Accordingly during the last years several papers have been devoted to compute the distribution of electric current and temperatures in electrodes (see for instance [2] and references therein). Most of them are based on cylindrical geometry and finite differences procedures.

Thermo-electrical modeling leads to a nonlinear system of partial differential equations for electromagnetic field and temperature. Coupling between Maxwell and heat transfer equations is due to Joule effect, which is the source term in the heat equation, and also to the fact that thermo-electrical parameters depend on temperature. As we already mentioned, Soderberg paste is non-conductive at room-temperature but it is a good conductor, similar to pure graphite, at the highest temperatures (about 2500°C).

A key point to solve this thermo-electrical model is to have a good 3D solver for the eddy currents problem arising from Maxwell equations in the low-frequency regime. This model should then be coupled with a thermal one.

A finite element method to solve the eddy currents problem in a bounded 3D-domain which contains not only the electrodes but the whole furnace is studied in [5]. However, the model presented in that paper is very complex and its numerical solution takes a lot of computer time. This is why it is useful to have simpler models to describe separate components of the whole system. In the present work, we study one such problem which consists of solving the eddy currents model in a domain including only one electrode (see Figure 1).

One of the main difficulties to study the problem in a bounded domain is defining mathematically suitable and physically realistic boundary conditions. Essential and natural boundary conditions are considered in [6] and [5]. However, these boundary conditions are not directly related with the physical data in the case of an electrode. In the present

paper, in order to deal with this question, we propose a finite element method to solve the eddy currents model in a bounded conductor domain by using the input current intensity as unique boundary data. We consider a formulation in terms of the magnetic field and impose the boundary conditions by means of Lagrange multipliers. We report numerical results which exhibit the good performance of the method.

## 2 THE EDDY CURRENTS PROBLEM

Eddy currents are usually modeled by the low-frequency harmonic Maxwell equations. We are interested in solving the problem in a bounded conductor domain  $\Omega$  crossed by an alternating electric current of angular frequency  $\omega$ . In this case, the model reduces to

$$\mathbf{curl} \mathbf{H} = \mathbf{J}, \quad (1)$$

$$i\omega\mu\mathbf{H} + \mathbf{curl} \mathbf{E} = \mathbf{0}, \quad (2)$$

$$\mathbf{J} = \sigma\mathbf{E}, \quad (3)$$

where  $\mathbf{H}$  is the magnetic field,  $\mathbf{J}$  the current density, and  $\mathbf{E}$  the electric field amplitudes. The coefficients  $\mu$  and  $\sigma$ , which correspond to the magnetic permeability and the electric conductivity, respectively, are not supposed to be constant in the whole  $\Omega$ , but we assume that there exist constants  $\underline{\mu}$ ,  $\bar{\mu}$ ,  $\underline{\sigma}$ , and  $\bar{\sigma}$  such that

$$0 < \underline{\mu} \leq \mu(\mathbf{x}) \leq \bar{\mu} \quad \text{and} \quad 0 < \underline{\sigma} \leq \sigma(\mathbf{x}) \leq \bar{\sigma} \quad \text{in } \Omega.$$

From (3) and (1) we obtain that

$$\mathbf{E} = \frac{1}{\sigma} \mathbf{curl} \mathbf{H}. \quad (4)$$

and by substituting this into (2), the model reduces to the following single equation for the complex field  $\mathbf{H}$  (see [5] for further details):

$$i\omega\mu\mathbf{H} + \mathbf{curl} \left( \frac{1}{\sigma} \mathbf{curl} \mathbf{H} \right) = \mathbf{0}. \quad (5)$$

The boundary  $\partial\Omega$  of the domain splits into two pieces  $\Gamma_E$  and  $\Gamma_C$ .  $\Gamma_E$  is the tip of the electrode where the electric arc arises. The rest of the electrode boundary splits in its turn as follows:  $\Gamma_C = \Gamma_C^0 \cup \Gamma_C^1 \cup \dots \cup \Gamma_C^{N_c}$ , where  $\Gamma_C^n$ ,  $n = 1, \dots, N_c$ , are the parts of the boundary connected to the wires supplying electric current to the electrode, and  $\Gamma_C^0$  the remaining (see Figure 1). We consider the case  $\Gamma_E \neq \emptyset$  and  $\Gamma_C^n \cap \Gamma_E = \emptyset$ ,  $n = 1, \dots, N_c$ .

The input current intensities through each wire,  $I_n$ ,  $n = 1, \dots, N_c$ , are known data, whereas no current goes through  $\Gamma_C^0$ . Hence we are led to impose the following boundary

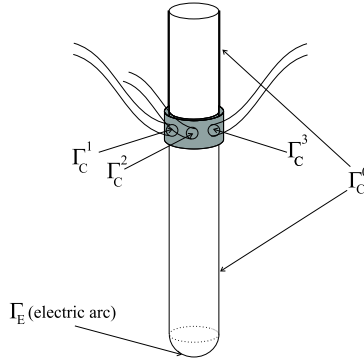


Figure 1: Sketch of one single electrode

conditions:

$$\int_{\Gamma_C^n} \mathbf{curl} \mathbf{H} \cdot \mathbf{n} = I_n \quad \text{on } \Gamma_C^n, \quad n = 1, \dots, N_c, \quad (6)$$

$$\mathbf{E} \times \mathbf{n} = \mathbf{0} \quad \text{on } \Gamma_C^n, \quad n = 1, \dots, N_c, \quad (7)$$

$$\mathbf{curl} \mathbf{H} \cdot \mathbf{n} = 0 \quad \text{on } \Gamma_C^0, \quad (8)$$

$$\mathbf{H} \cdot \mathbf{n} = 0 \quad \text{on } \Gamma_C. \quad (9)$$

On the other hand, the natural boundary condition corresponding to free current exit on the electrode tip yields

$$\mathbf{E} \times \mathbf{n} = \mathbf{0} \quad \text{on } \Gamma_E. \quad (10)$$

Conditions (7) and (9) turn out to be natural boundary conditions of the weak formulation of the problem, when (6) and (8) are imposed by Lagrange multiplier techniques. Hence they can be considered as complementary boundary conditions which are needed to get uniqueness of solution.

### 3 WEAK FORMULATION

To obtain a weak formulation of the boundary value problem (5)–(10) in terms of the magnetic field, we notice that the boundary conditions (9)–(10) imply that the tangential component of  $\mathbf{E}$  on the boundary of  $\Omega$  is a gradient. In particular, we obtain by formal calculus that  $\mathbf{E} \times \mathbf{n} = \nabla \phi \times \mathbf{n}$  on  $\partial\Omega$  for some scalar function  $\phi$  with  $\phi = 0$  on  $\Gamma_E$ . Then, multiplying the equation (5) by a test function  $\mathbf{G}$  such that  $\mathbf{curl} \mathbf{G} \cdot \mathbf{n} = 0$  on  $\Gamma_C$ , and using a Green's formula and (4), we obtain

$$i\omega \int_{\Omega} \mu \mathbf{H} \cdot \bar{\mathbf{G}} + \int_{\Omega} \frac{1}{\sigma} \mathbf{curl} \mathbf{H} \cdot \mathbf{curl} \bar{\mathbf{G}} = 0.$$

Let  $\mathcal{X}$  be the space of vector fields defined in  $\Omega$  which are square-integrable and have a square-integrable curl. Namely,

$$\mathcal{X} := \left\{ \mathbf{G} : \Omega \longrightarrow \mathbb{C}^3 : \int_{\Omega} |\mathbf{G}|^2 < \infty \text{ and } \int_{\Omega} |\mathbf{curl} \mathbf{G}|^2 < \infty \right\}.$$

We denote by  $\|\cdot\|$  the natural norm of this space defined by

$$\|\mathbf{G}\| := \left( \int_{\Omega} |\mathbf{G}|^2 + \int_{\Omega} |\mathbf{curl} \mathbf{G}|^2 \right)^{1/2}. \tag{11}$$

Let  $a$  be the sesquilinear continuous and elliptic form defined on  $\mathcal{X}$  by

$$a(\mathbf{H}, \mathbf{G}) := i\omega \int_{\Omega} \mu \mathbf{H} \cdot \bar{\mathbf{G}} + \int_{\Omega} \frac{1}{\sigma} \mathbf{curl} \mathbf{H} \cdot \mathbf{curl} \bar{\mathbf{G}}.$$

Let

$$\tilde{I} := \begin{cases} \frac{I_n}{\text{meas}(\Gamma_c^n)} & \text{on } \Gamma_c^n, \quad n = 1, \dots, N_c, \\ 0 & \text{on } \Gamma_c^0, \end{cases}$$

and consider the following linear manifold of  $\mathcal{X}$ :

$$\mathcal{W}(\tilde{I}) := \left\{ \mathbf{G} \in \mathcal{X} : \int_{\Gamma_c} \mathbf{curl} \mathbf{G} \cdot \mathbf{n} \nu = \int_{\Gamma_c} \tilde{I} \nu, \quad \forall \nu : \nu|_{\Gamma_c^n} = \text{constant}, \quad n = 1, \dots, N_c \right\}.$$

Notice that, in particular,

$$\mathcal{W}(0) = \left\{ \mathbf{G} \in \mathcal{X} : \int_{\Gamma_c} \mathbf{curl} \mathbf{G} \cdot \mathbf{n} \nu = 0, \quad \forall \nu : \nu|_{\Gamma_c^n} = \text{constant}, \quad n = 1, \dots, N_c \right\}.$$

Then, the following is a variational formulation of the boundary value problem (5)–(10):

Find  $\mathbf{H} \in \mathcal{W}(\tilde{I})$  satisfying

$$a(\mathbf{H}, \mathbf{G}) = 0 \quad \forall \mathbf{G} \in \mathcal{W}(0). \tag{12}$$

This problem has a unique solution. Indeed, this is an immediate consequence of the facts that  $a$  is elliptic in  $\mathcal{W}(0)$  and  $\mathcal{W}(\tilde{I})$  is a non-empty closed convex manifold.

To avoid dealing with functions satisfying the constraints associated with  $\mathcal{W}(\tilde{I})$ , we consider a mixed formulation of this problem. It consists of handling the boundary conditions (6) and (8) in a weak sense by introducing a Lagrange multiplier defined on  $\Gamma_c$ .

Let

$$\mathcal{L} := \left\{ \nu : \Gamma_c \longrightarrow \mathbb{C} : \nu|_{\Gamma_c^n} = \text{constant}, \quad n = 1, \dots, N_c \right\}.$$

Let  $b$  be the bilinear form defined on  $\mathcal{X} \times \mathcal{L}$  by

$$b(\mathbf{G}, \lambda) := \int_{\Gamma_c} \mathbf{curl} \mathbf{G} \cdot \mathbf{n} \lambda.$$

Then, the mixed problem associated with (12) is the following one:

Find  $\mathbf{H} \in \mathcal{X}$  and  $\lambda \in \mathcal{L}$  satisfying

$$a(\mathbf{H}, \mathbf{G}) + b(\bar{\mathbf{G}}, \lambda) = 0 \quad \forall \mathbf{G} \in \mathcal{X}, \tag{13}$$

$$b(\mathbf{H}, \bar{\nu}) = \int_{\Gamma_c} \tilde{I} \bar{\nu} \quad \forall \nu \in \mathcal{L}. \tag{14}$$

An inf-sup condition for the bilinear form  $b$  can be proved by using results concerning vector potentials in  $\mathbb{R}^3$  (see [7]). Then, as a consequence of the classical Babuška-Brezzi theory, we know that the problem above attains a unique solution.

From the physical point of view, the Lagrange multiplier  $\lambda$  is a sort of surface potential of the tangential component of the electric field  $\mathbf{E}$  on the boundary of the conductor domain; in fact, it can be proved that  $\mathbf{E} \times \mathbf{n} = -\nabla \lambda \times \mathbf{n}$  on  $\Gamma_c$ .

#### 4 FINITE ELEMENT SOLUTION

We consider a shape-regular tetrahedral mesh  $\mathcal{T}_h$  of  $\Omega$  where, as usual,  $h$  denotes the corresponding mesh-size.

Since the magnetic field is a vector field of  $\mathcal{X}$ , it will be discretized by using the Nédélec edge finite element space (see [8]):

$$\mathcal{X}_h := \{ \mathbf{G}_h \in \mathcal{X} : \mathbf{G}_h(\mathbf{x}) = \mathbf{a} \times \mathbf{x} + \mathbf{b}, \mathbf{a}, \mathbf{b} \in \mathbb{C}^3, \mathbf{x} \in K, \forall K \in \mathcal{T}_h \}.$$

An explicit computation shows that the vector fields of the form  $\mathbf{a} \times \mathbf{x} + \mathbf{b}$  have constant tangential components along each straight line. Moreover, given a tetrahedron  $K \in \mathcal{T}_h$  and any six complex numbers  $\beta_n$ ,  $n = 1 \dots 6$ , there exists a unique vector field of this form (i.e., unique  $\mathbf{a}, \mathbf{b} \in \mathbb{C}^3$ ) such that its tangential component along the  $n$ -th edge of  $K$  coincide with  $\beta_n$  for  $n = 1 \dots 6$ , respectively. Thus, these tangential components along the edges of  $K$  for each  $K \in \mathcal{T}_h$  can be taken as the degrees of freedom defining the vector fields of  $\mathcal{X}_h$ .

These elements are  $\mathcal{X}$ -conforming in the sense that,  $\forall \mathbf{G}_h \in \mathcal{X}_h$ , their tangential traces on each triangular face  $T$  of  $K$  only depend on the degrees of freedom of  $\mathbf{G}_h$  on the three edges of  $T$ . Hence, these elements are piecewise linear vector fields with tangential traces that are continuous through the faces of the mesh.

On the other hand, for the Lagrange multiplier we will use the finite element space

$$\mathcal{L}_h := \left\{ \lambda_h \in \mathcal{Q}_h^1 : \lambda_h|_{\Gamma_c^n} = \text{constant}, n = 1, \dots, N_c \right\},$$

where  $Q_h^1$  is the space of piecewise linear continuous functions defined on the triangular mesh  $\mathcal{T}_h^{\Gamma_C}$ , induced by  $\mathcal{T}_h$  on the polyhedral surface  $\Gamma_C$ .

Thus, we obtain the following discrete problem:

Find  $\mathbf{H}_h \in \mathcal{X}_h$  and  $\lambda_h \in \mathcal{L}_h$  satisfying

$$\begin{aligned} a(\mathbf{H}_h, \mathbf{G}_h) + b(\bar{\mathbf{G}}_h, \lambda_h) &= 0 \quad \forall \mathbf{G}_h \in \mathcal{X}_h, \\ b(\mathbf{H}_h, \bar{\nu}_h) &= \int_{\Gamma_C} \tilde{I} \bar{\nu}_h \quad \forall \nu_h \in \mathcal{L}_h. \end{aligned}$$

If the solution  $\mathbf{H}$  of (13)–(14) is smooth enough, then this discrete problem attains a unique solution  $(\mathbf{H}_h, \lambda_h)$  which satisfies

$$\|\mathbf{H} - \mathbf{H}_h\| = \left( \int_{\Omega} |\mathbf{H} - \mathbf{H}_h|^2 + \int_{\Omega} |\mathbf{curl} \mathbf{H} - \mathbf{curl} \mathbf{H}_h|^2 \right)^{1/2} \leq Ch.$$

Indeed, we can first prove that the problem is well posed, and then obtain the estimate by following similar arguments to those developed in the proof of Theorem II.1.1 in [7]. For that, we need to prove that the finite-dimensional space analogue to  $\mathcal{W}(\tilde{I})$  is non empty.

The inequality above provides error estimates for the curl of the magnetic field  $\mathbf{H}$ , which allows to compute the variables of interest in most applications:  $\mathbf{E}$  and  $\mathbf{J}$ . To obtain error estimates for the electric surface potential  $\lambda$ , a discrete inf-sup condition would be needed. However, the constant corresponding to this discrete inf-sup condition does not seem to remain bounded away from zero when  $h$  goes to 0. Actually, by means of numerical experiments, we have observed that this constant converges to zero with a linear dependence on  $h$ . In spite of this, the numerical experiments reported in the following section show a double order of convergence for the variable  $\lambda$ .

## 5 NUMERICAL EXPERIMENTS

In this section we present some numerical results obtained with a MATLAB code which implements the finite element method described above. In order to validate the computer code and to test the performance and convergence properties of the method, we have applied it to a particular problem with known analytical solution: the eddy-currents problem in a cylindrical domain  $\Omega$ , of radius  $R$  and height  $L$ , which is a bounded section of an infinite cylinder (see Figure 2).

We consider an alternating current  $\mathbf{J}$  going through the conductor  $\Omega$  in the direction of its axis. This current is assumed to be axially symmetric with an intensity  $I(t) = I_0 \cos \omega t$ . Concerning the physical properties, the electric conductivity  $\sigma$  and the magnetic permeability  $\mu$  are taken as constants in  $\Omega$ .

We have taken the bottom surface of the cylinder as the free current exit boundary  $\Gamma_E$ , its lateral surface as  $\Gamma_C^0$ , and its top as the input current boundary  $\Gamma_C^1$ . We have used the input current intensity through  $\Gamma_C^1$  as the unique boundary data.

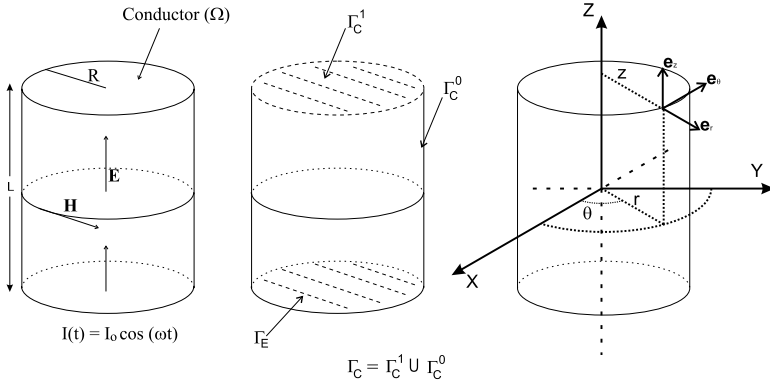


Figure 2: Sketch of the domain. Coordinate system.

To obtain the analytical solution of this problem we use a cylindrical coordinate system  $(r, \theta, z)$  with the  $z$ -axis coinciding with the axis of the cylinder (see Figure 2). We denote  $\mathbf{e}_r$ ,  $\mathbf{e}_\theta$ , and  $\mathbf{e}_z$  the unit vectors in the corresponding coordinate directions.

Because of the assumed conditions on  $\mathbf{J}$ , only the  $z$ -component of the electric field  $\mathbf{E}$  does not vanish in the conductor. Moreover, it depends on the radial coordinate  $r$ , but is independent of the other two coordinates  $\theta$  and  $z$ . Consequently, only the  $\theta$ -component of the magnetic field  $\mathbf{H} = \frac{i}{\omega\mu} \mathbf{curl} \mathbf{E}$  does not vanish and it also depends only on the coordinate  $r$ . Then, taking into account the expression of the  $\mathbf{curl}$  operator in cylindrical coordinates, straightforward computations allow us to obtain the following expression for the magnetic field (see [5] for details):

$$\mathbf{H}(r, \theta, z) = \frac{I_0}{2\pi R} \frac{\mathcal{I}_1(\gamma r)}{\mathcal{I}_1(\gamma R)} \mathbf{e}_\theta, \quad r \in (0, R), \quad \theta \in [0, 2\pi], \quad z \in \mathbb{R}.$$

where  $\mathcal{I}_1$  is the modified Bessel function of the first kind and order 1, and  $\gamma = \sqrt{i\omega\mu\sigma} \in \mathbb{C}$ .

On the other hand, since  $\mathbf{E} \times \mathbf{n} = -\nabla\lambda \times \mathbf{n}$  on  $\Gamma_C$ , by using the expression of the gradient operator in cylindrical coordinates, we obtain the following analytical expression for the Lagrange multiplier  $\lambda$  on  $\Gamma_C$ :

$$\lambda(r, \theta, z) = -z E_z(R, \theta, z) = -z E_z(R).$$

Notice that  $\lambda$  is constant on the top surface  $\Gamma_C^1$  and it depends only on  $z$  on the lateral surface  $\Gamma_C^0$ .

We have used the following geometrical and physical data:

- $R = 0.5$  m;

- $L = 1$  m;
- $\sigma = 10^6 (\Omega\text{m})^{-1}$ ;
- $\mu = \mu_0 = 4\pi \cdot 10^{-7} \text{ Hm}^{-1}$  (magnetic permeability of free space);
- $I_0 = 7 \times 10^4$  A;
- $\omega = 50$  Hz.

To determine the order of convergence, the numerical method has been used on several successively refined meshes and we have compared the obtained numerical solutions with the analytical one. Figure 3 shows the coarsest mesh used for the domain.

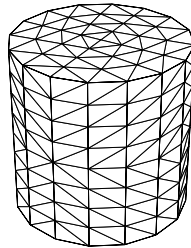


Figure 3: Coarsest mesh on the conductor domain.

We report in Table 1 the numerical results obtained on several meshes for the magnetic field  $\mathbf{H}$ . The table includes the mesh-size, the number of degrees of freedom (d.o.f.), the norm defined in (11) of the computed solution and its corresponding error, and the percent relative error. Table 2 shows similar results for the electric surface potential  $\lambda$ .

Table 1: Norms of computed solution and errors for the magnetic field  $\mathbf{H}$ .

Mesh-size	Number d.o.f.	Computed solution	Error	Rel. Error (%)
$h$	2096	139186.29	71145.95	51.12
$h/2$	15520	150109.42	44590.87	29.71
$h/3$	51024	152098.30	31208.13	20.52
$h/4$	119360	152784.39	23810.03	15.58

Figures 4 and 5 show log-log plots of the errors for the magnetic field and the electric surface potential, respectively, versus the number of d.o.f. for the same meshes. A linear dependence on the mesh-size for  $\mathbf{H}$  and a quadratic dependence for  $\lambda$  can be clearly observed in these graphs.

Table 2: Norms of computed solution and errors for the electric surface potential  $\lambda$ .

Mesh-size	Number d.o.f.	Computed solution	Error	Rel. error (%)
$h$	2096	0.4013	0.1539	38.35
$h/2$	15520	0.4052	0.0470	11.60
$h/3$	51024	0.4059	0.0215	5.30
$h/4$	119360	0.4061	0.0122	3.00

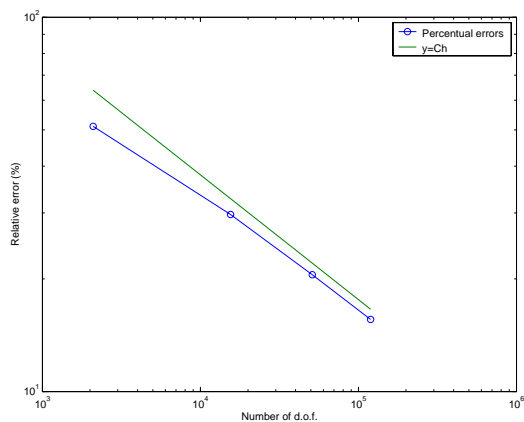


Figure 4: Error curve for the magnetic field  $\mathbf{H}$  (log-log scale).

## REFERENCES

- [1] A. Bossavit. *Computational Electromagnetism. Variational Formulations, Complementarity, Edge Elements*. Academic Press, (1998).
- [2] A. Bermúdez, J. Bullón, and F. Pena. A finite element method for the thermoelectrical modelling of electrodes. *Comm. Numer. Methods Engrg.*, **14**, 581–593 (1998).
- [3] R. Innvær and L. Olsen. Practical use of mathematical models for Soderberg electrodes. *Elkem Carbon Technical Paper presented at the A.I.M.E. Conference*, (1980).
- [4] J. Bullón and V. Gallego. New electrode for silicon metal production. *Electric Furnace Conference*, Nashville, (1994).
- [5] A. Bermúdez, R. Rodríguez, and P. Salgado. A finite element method with Lagrange multipliers for low-frequency harmonic Maxwell equations. *SIAM J. Numer. Anal.*, (to appear).
- [6] A. Alonso and A. Valli. A domain decomposition approach for heterogeneous time-

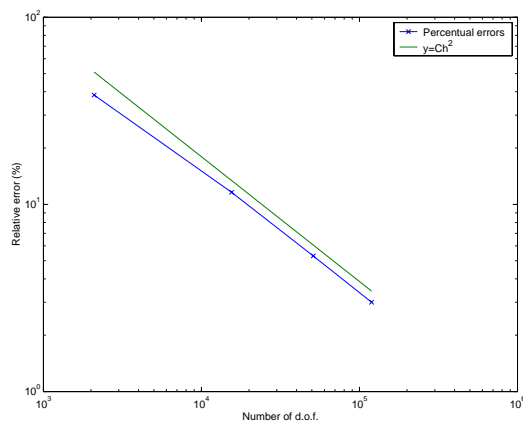


Figure 5: Error curve for the electric surface potential  $\lambda$  (log-log scale).

harmonic Maxwell equations. *Comput. Methods Appl. Mech. Engrg.*, **143**, 97–112 (1997).

- [7] V. Girault and P. A. Raviart. *Finite Element Methods for Navier-Stokes Equations. Theory and Algorithms*. Springer-Verlag, (1986).
- [8] J. C. Nédélec. Mixed finite elements in  $\mathbb{R}^3$ . *Numer. Math.*, **35**, 315–341 (1980).